

UNDERSTANDING THE CHLORINE ISOTOPIC COMPOSITION OF APATITES IN LUNAR BASALTS.

N. J. Potts^{1,2*}, R. Tartèse¹, I. A. Franchi¹, M. Anand^{1,3}. ¹Department of Physical Sciences, The Open University, Milton Keynes, UK. (*nicola.potts@open.ac.uk). ²Faculty of Earth and Life Sciences, VU University Amsterdam, Amsterdam, NL. ³Department of Earth Sciences, The Natural History Museum, London, UK.

Introduction: On Earth $\delta^{37}\text{Cl} = \sim 0 \pm 5 \text{ ‰}$ [1]. For lunar rocks elevated $\delta^{37}\text{Cl}$ values of up to 35 ‰ have been reported in apatites [1,2]. The initial study interpreted the elevated $\delta^{37}\text{Cl}$ in lunar rocks as a result of metal chlorides degassing in low- H_2O environments [1]. Additional data [3,4] have shown high- $\delta^{37}\text{Cl}$ values in samples with apatite containing appreciable amounts of H_2O (>2000 ppm). Metasomatism is thought to have fractionated Cl isotopes toward heavy $\delta^{37}\text{Cl}$ values in sample 79215 [2]. This process, however, is not thought to be widespread on the Moon and cannot account for the fractionation seen in other samples for which data are available, particularly mare basalts. Here we report preliminary measurements of $\delta^{37}\text{Cl}$ in apatites from lunar impact “melt rock” sample 14073,9. Results are compared with literature $\delta^{37}\text{Cl}$ data on lunar apatites to evaluate the effects impact processes may have had on $\delta^{37}\text{Cl}$ values. We then explore a potential scenario of the elevated $\delta^{37}\text{Cl}$ signature of the Moon.

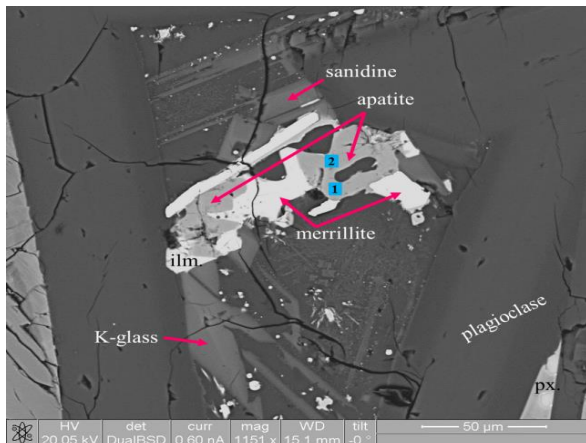


Figure 1: BSE image of 14073,9. Blue spots (not to scale) correspond to NanoSIMS analysis locations for apatite #12.

Sample petrogenesis: 14073 was initially classified as a KREEP basalt due to its high REE content [5]. There are similarities in trace element abundances between 14073, and Apollo 14 soils and breccias. This, along with high Ni and Ir contents and the presence of Fe-Ni-P-S melt globules, led to its description as a “melt rock” [6]. It consists of euhedral plagioclase laths (~50% modal abundance) with interstitial anhedral pyroxenes (~25% clinopyroxene; ~20% orthopyroxene) with minor ilmenite (~2%), and a late-stage mesostasis [7]. The mesostasis regions of 14073,9 are

composed of apatite, merrillite, fayalite, sanidine, and K-Ba-rich glass.

Methods: Apatite grains were identified, initially using SEM-derived X-ray maps and BSE images, followed by $^{16}\text{O}^1\text{H}$ and ^{35}Cl secondary ion images using the real-time imaging mode of the Cameca NanoSIMS 50L ion probe. For NanoSIMS measurements, a Cs^+ primary beam of 560 pA with an accelerating voltage of 16 kV was rastered on the sample surface over $25 \times 25 \mu\text{m}$ areas for 1 minute to pre-sputter and clean the sample surface. Areas of $8 \times 8 \mu\text{m}$ were then rastered for a further minute with a 90 pA beam current. Finally, analyses were carried out on $4 \times 4 \mu\text{m}$ areas with a 40 pA beam current. Secondary ions of $^{16}\text{O}^1\text{H}$, ^{18}O , ^{28}Si , ^{35}Cl , ^{37}Cl , and $^{40}\text{Ca}^{19}\text{F}$ were collected simultaneously on electron multipliers for ~7 minutes. Cl and OH abundances were calibrated using the $^{35}\text{Cl}/^{18}\text{O}$ and $^{16}\text{O}^1\text{H}/^{18}\text{O}$ ratios measured on reference apatites standards [8]. Abundance errors are low for both Cl (30 – 60 ppm) and H_2O (17 – 22 ppm). Due to its high abundance and high ionisation efficiency, F abundances could not be measured directly on an electron multiplier and were calculated by difference ($\text{F} = (1 - (\text{Cl} + \text{OH})) \text{ apfu}$). The same standards used to calibrate abundances were used to correct measured $^{37}\text{Cl}/^{35}\text{Cl}$ ratios for instrumental mass fractionation (IMF). The $^{37}\text{Cl}/^{35}\text{Cl}$ ratios are given here in the standard delta notation calibrated against the $^{37}\text{Cl}/^{35}\text{Cl}$ ratio for Standard Mean Ocean Chloride (SMOC). Errors shown are 2σ .

Results: Four $\delta^{37}\text{Cl}$ values, from 3 apatites, are reported here. The apatite grain (#12) in which 2 analyses were carried out, is shown in Figure 1. $\delta^{37}\text{Cl}$ values within this grain are appreciably different with values of $+5.0 \pm 2.7 \text{ ‰}$ and $+14.8 \pm 2.6 \text{ ‰}$, demonstrating a large variation in $\delta^{37}\text{Cl}$ values within a single apatite grain. The Cl concentrations measured at the two spots vary by more than a factor of 2 (1812 and 4006 ppm, respectively), and broadly similar H_2O contents of 782 and 1102 ppm, respectively. Figure 2 shows that there is no obvious relationship between $\delta^{37}\text{Cl}$ and H_2O content in the analysed apatites, while there is a positive correlation between Cl content and $\delta^{37}\text{Cl}$ ($R^2 = 0.99$). This may, however, be a reflection of the small variation in H_2O content. In terms of $\delta^{37}\text{Cl}$ vs. Cl concentration, apatites in 14073,9 plot within similar regions to basalts from [1,3] and an isolated apatite grain found within the matrix of lunar meteorite

breccia Northwest Africa (NWA) 4472 [4]. Cl concentrations in apatites from [1] are all higher than those measured in [3] and this study. The apatites from [1] also have the highest $\delta^{37}\text{Cl}$ value measured from mare basalts thus far. The majority of Cl concentrations from [3] are lower than values measured in this study.

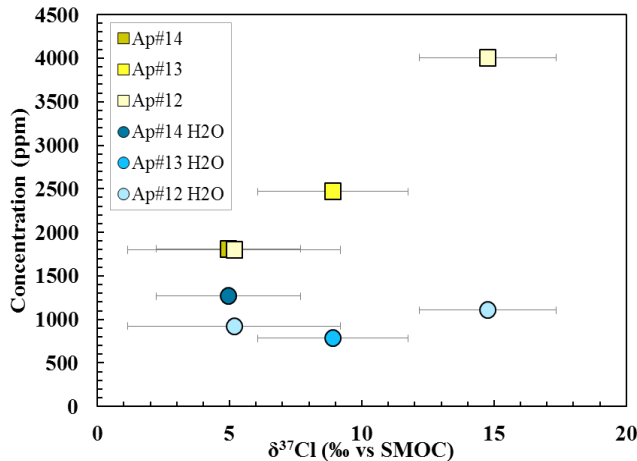


Figure 2: $\delta^{37}\text{Cl}$ versus Cl (yellow squares) and H_2O (blue circles) concentrations for apatites in 14073,9.

Discussion: There appears to be no relationship between the bulk geochemistry of the basalts and $\delta^{37}\text{Cl}$ values in the literature data. As the results of 14073,9 are indistinguishable from mare basalts, impact processes do not appear to have influenced Cl concentrations or $\delta^{37}\text{Cl}$ values in this sample. Further data, however, are required to determine whether this sample retains initial magmatic signatures.

The results of [3] showed the variability of $\delta^{37}\text{Cl}$ values within a lunar sample. This demonstrated that multiple apatites should be measured when investigating Cl isotopes. The data from the current study show that $\delta^{37}\text{Cl}$ values and Cl concentrations can vary greatly within one grain over a 10 μm distance. Multiple analyses, preferably both concentration and isotopic measurements on the same spot, from a number of apatites per sample are desirable for an accurate assessment of indigenous Cl isotope signatures.

Apatite data from 14073,9 and [1] appear to show a general trend between increasing Cl concentrations and increasing $\delta^{37}\text{Cl}$ values ($R^2 = 0.92$). More data are required to quantify potential trends between Cl concentration and $\delta^{37}\text{Cl}$ values. If these trends are robust then a process which simultaneously increases Cl concentration and ^{37}Cl is required [or vice versa]. Based on the data presented in Figure 1, this process does not appear to be strongly linked to changes in apatite water contents. Preferential degassing of the lighter ^{35}Cl would reduce the Cl concentration and, as such, the opposite trend would be expected if this were the main

process affecting Cl isotope fractionation [9]. Observations from [3] indicate a potential mixing trend between $\delta^{37}\text{Cl}$ -elevated highlands samples and relatively $\delta^{37}\text{Cl}$ -depleted lunar basalts.

Isotopically heavy $\delta^{37}\text{Cl}$ values and high Cl concentrations in apatites from lunar highlands samples could represent initial Moon Cl values. A process, however, that enriches Moon-forming material in heavy ^{37}Cl relative to the Earth would be required for this scenario (based on the assumption of the Moon being formed from BSE-type material). A study on Earth's Cl depletion relative to chondritic material [10] suggests preferential loss of heavy halogens during planetary accretion as a possible scenario. Large impactors, such as a giant Moon-forming impact [10], result in preferential loss of a Cl-rich veneer from Earth. During accretion of the Moon, and subsequent outgassing, the lighter ^{35}Cl would be preferentially lost to space [1] which would also significantly reduce the bulk-Cl content of the Moon. A similar hypothesis was initially discarded by [1] from a lack of supporting evidence from other volatiles such as K. This volatile enrichment in the Moon, however, would be expected for only the heavy halogens such as Cl, I, and Br [10].

It is unknown, however, what process(es) could further fractionate Cl isotope signatures of mare source regions as apatites in mare basalts appear to have relatively lighter Cl isotope signatures compared to the highlands samples. A better understanding of other petrological influences in modifying the Cl isotopic signatures of lunar samples is required to further address this issue. Ongoing work aims to acquire additional data for $\delta^{37}\text{Cl}$ from analyses of multiple grains within a sample to provide further insight into any variability of $\delta^{37}\text{Cl}$ values in mare basalts as per their geochemistry, age, depth burial, etc. These measurements will ultimately help improve our understanding of the significance of the heavy $\delta^{37}\text{Cl}$ signatures of lunar apatites and their potential implications for the history of water in the lunar interior.

Acknowledgements: We thank NASA CAPTEM for allocation of Apollo samples. This work was funded by an STFC Studentship awarded to NJP and research grant to MA (Grant no. ST/I001298/1). Francis McCubbin is thanked for providing apatite standards.

References: [1] Sharp, Z.D. et al. (2010) *Science*, 329, 1050-1053. [2] Treiman, A.H. et al. (2014) *Am. Min.* 99, 1860-1870. [3] Boyce, J.W. et al. (2013) *LPSC*, 44th, #2851. [4] Tartèse, R. et al. (2014), *MaPS*, 49, 2266-2289. [5] El Goresy, A. et al. (1971) *EPSL*, 13, 121-129. [6] Schonfed, E., Meyer, C. (1972) 3rd Lunar Sci. Conf. 1681-1691. [7] Gancarz, A.L., et al. (1971) *EPSL*, 12, 1-18. [8] McCubbin F.M. et al. (2012) *Geol.*, 40, 683-686. [9] Hauri E.H. et al. (2015) *EPSL*, 409, 252-264. [10] Sharp, Z.D., et al. (2013) *EPSL*, 369-370, 71-77.